Electronic Supplementary Material (ESI) for Physical Chemistry Chemical Physics.

Supporting information

Covalently linked pyrene antennas for optically dense yet aggregation-resistant light-harvesting systems

Lubna Salah[a], Saad Makhseed[a], Basma Ghazal[b], Ahmed Abdel Nazeer[c], Marc K. Etherington[d], Carlito S. Ponseca Jr[e], Chunyong Li[f], Andrew P. Monkman[f], Andrew Danos[f,]* Ali Shuaib[g,]*

[a] Department of Chemistry, Faculty of Science, Kuwait University, P.O. Box 5969, Safat-13060, Kuwait.

[b] National Research Centre-NRC-Egypt Organometallic and Organometalloid Chemistry, Giza, Egypt

[c] Nanotechnology and Advanced Materials Program, Energy & Building Research Center, Kuwait Institute for Scientific Research (KISR), P.O Box 24885, Safat, 13109, Kuwait.

[d] Department of Mathematics, Physics & Electrical Engineering, Northumbria University, Ellison Place, Newcastle upon Tyne, NE1 8ST, UK.

[e] Mathematics and Natural Science Department, Gulf University for Science and Technology, Kuwait.

[f] Department of Physics, Durham University, South Road, Durham, DH1 3LE, UK

[g] Biomedical Engineering Unit, Department of Physiology, Faculty of Medicine, Kuwait University, P.O. Box 24923, Safat-13110, Kuwait

*Corresponding Authors

Email address: Andrew Danos: andrew.danos@durham.ac.uk
Ali Shuaib: ali.shuaib@ku.edu.kw

1. Synthesis

In a previous study[1], the synthesis of a zinc(II) phthalocyanine-pyrene conjugate (**ZnPcPy**) was explored using two approaches: (i) traditional cyclization of pyrene-modified Pc subunit 2 in Zn(II) ions, and (ii) coupling multiple azido pyrene derivatives to a custom alkyne-terminated macrocyclic platform Pc1 via CuAAC. The traditional method failed due to steric hindrance preventing cyclization. In contrast, the molecular platform approach successfully synthesized the **ZnPcPy** with high yields (>80%). The structure was characterized using NMR, FT-IR, MALDI-TOF, and CHN elemental analysis, confirming its chemical composition and the formation of the compound.

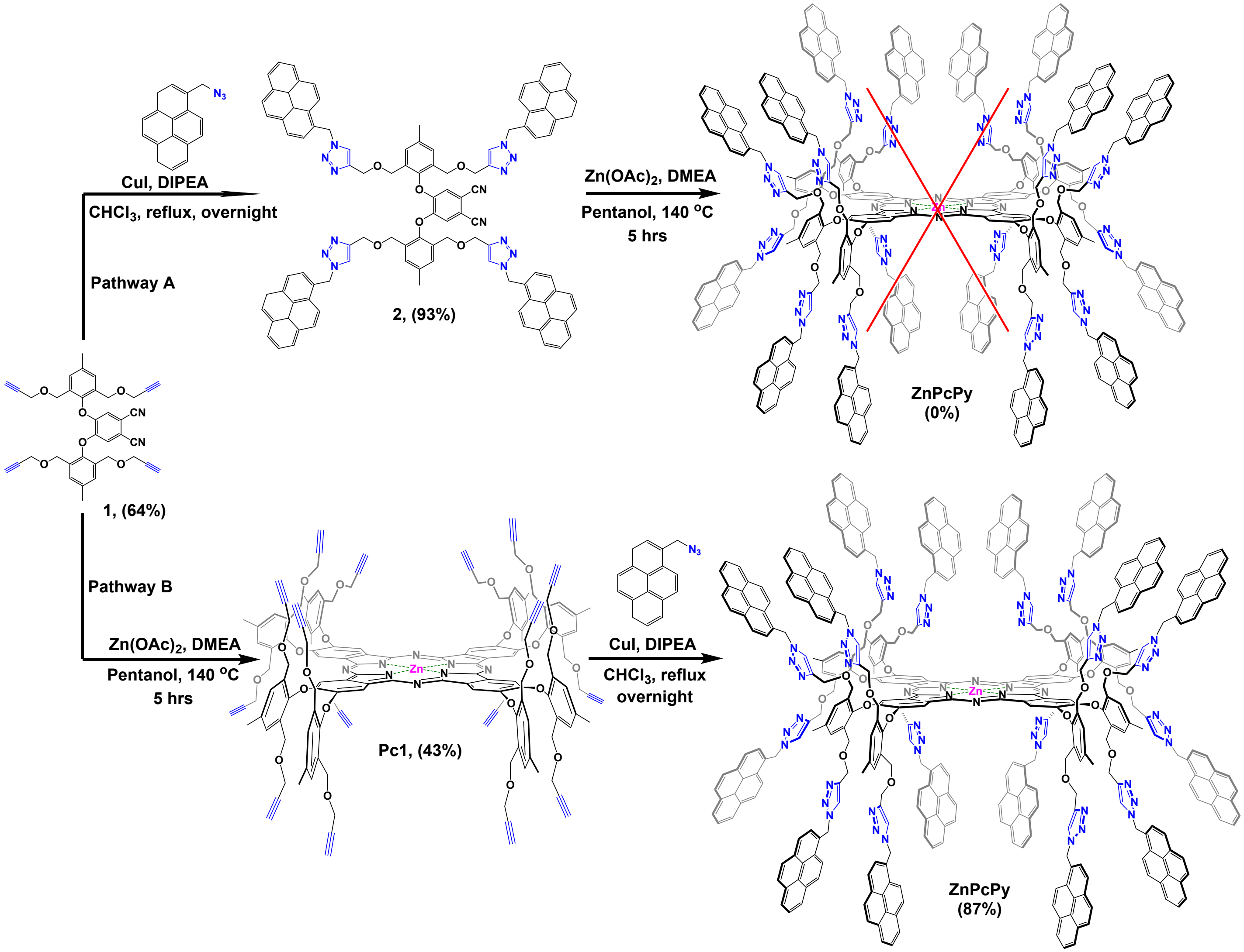

Scheme 1: Synthesis of multivalent Pyrene-Containing zinc(II) Phthalocyanine (**ZnPcPy**) via Pathway A, the Traditional Synthetic Method, and Pathway B, the Molecular Platform Approach.

2. Absorption study

The UV-Vis spectra of **ZnPcPy** were performed in three distinct solvents: Chloroform ($CHCl_3$), Dimethylformamide (DMF), and Tetrahydrofuran (THF), with investigations of the emission spectra performed at two excitation wavelengths: 345 nm and 615 nm in THF. The absorption spectra of **ZnPcPy** revealed the presence of characteristic bands corresponding to conjugated phthalocyanine (**ZnPc**) at 684 nm and pyrene (**Py**) at 310 nm, 330 nm, and 345 nm. These bands provide insights into the optical properties of the **ZnPcPy** complex and its individual components, as depicted in **Figure S1**.

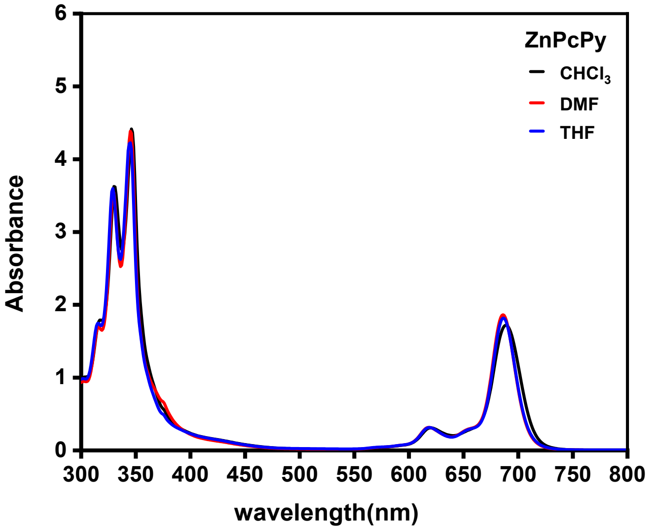

Figure S1: UV-Vis spectra of **ZnPcPy** in various solvents ($CHCl_3$, DMF, and THF).

To assess aggregation, the study employed the Lambert-Beer Law, examining a range of concentrations from 10 µM to 1 µM (**Figure S2**). The results indicated no evidence of aggregation formation within the investigated concentration range.

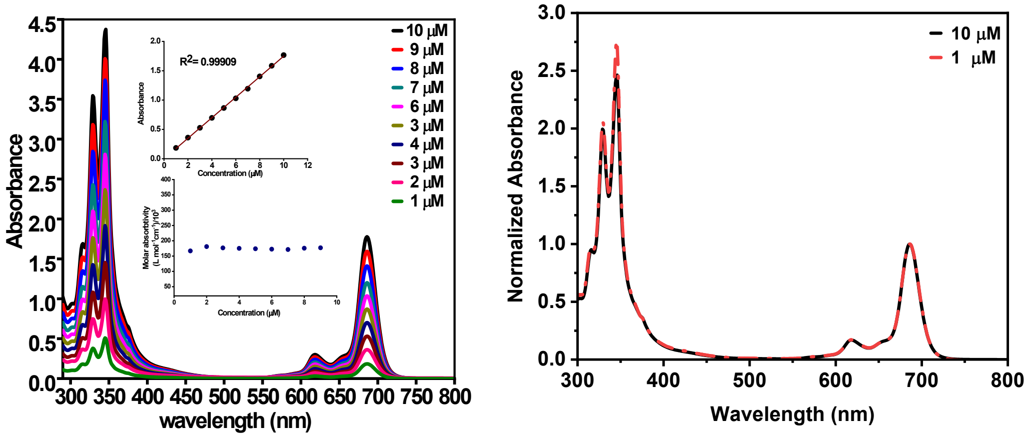

Figure S2: Absorption spectra of **ZnPcPy** at concentration range 10 µM to 1 µM (left), and comparison of normalized absorption spectra (right) indicating no formation of aggregates.

3. Emission study

Figure S3 demonstrates the behavior of **ZnPcPy** in THF solvent upon excitation with light at two different wavelengths, 345 nm and 615 nm. Specifically, under excitation with 345 nm light, **ZnPcPy** displays a negligible contribution from the **Py** band at approximately 400 nm.

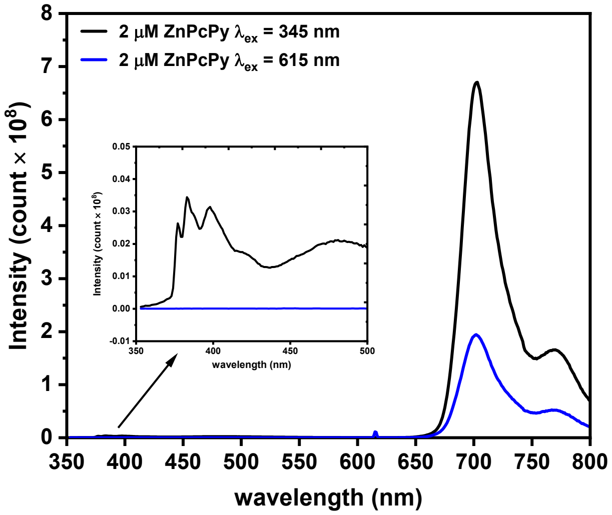

Figure S3: Emission spectra of **ZnPcPy** in THF solvent excited at 345 nm and 615 nm.

In **Figure S4,** the emission spectra for **ZnPc**, **MePy**, and **ZnPcPy** are presented for excitation wavelengths of 345 nm and 615 nm in both $CHCl_3$ and DMF solvents.

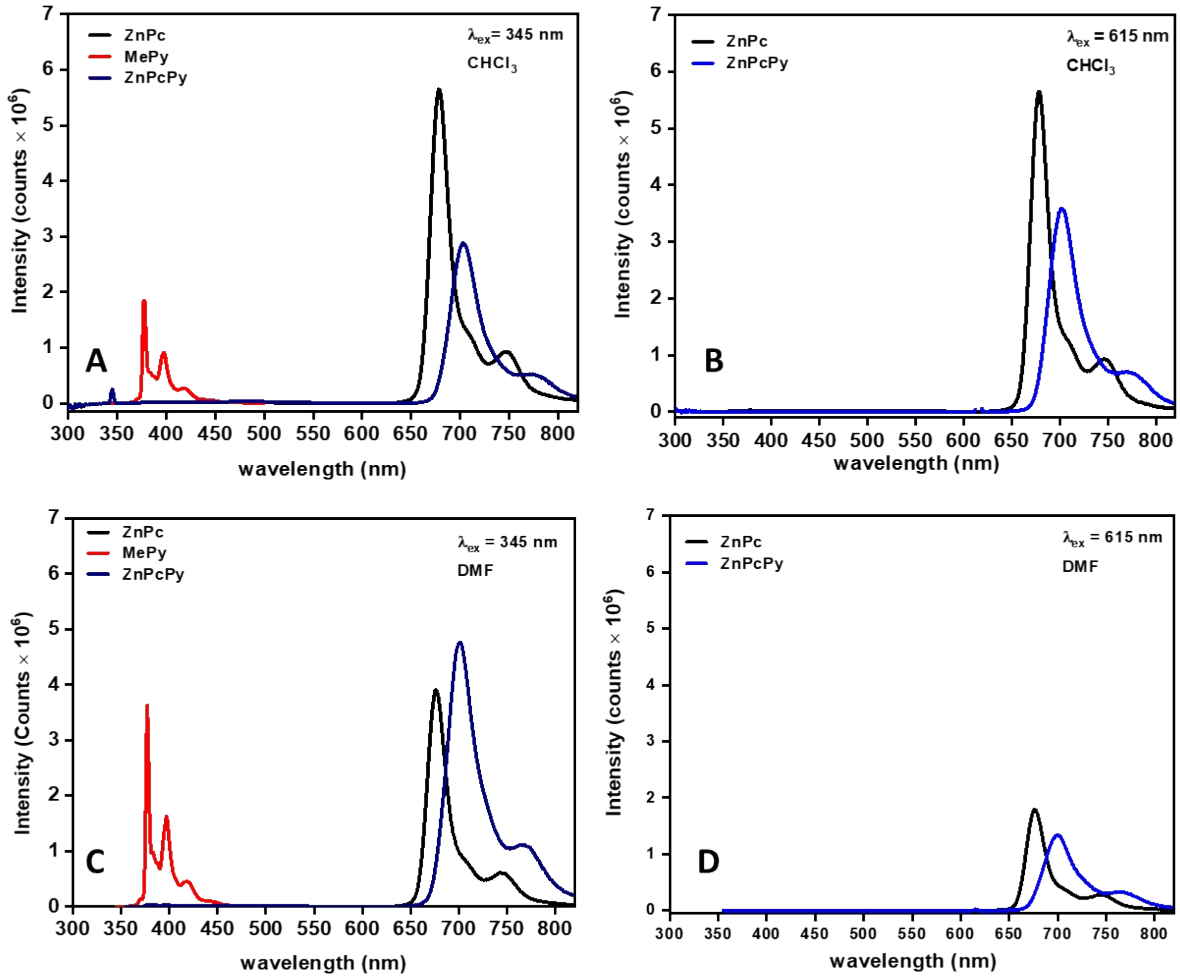

Figure S4: Emission spectra of **ZnPc** (Black), **MePy** (Red), and **ZnPcPy** (Blue), upon excitation at wavelengths of 345 nm (**A**-**C**) and 615 nm (**B**-**D**). Panels **A** and **B** display the respective emission spectra in the CHCl$_3$ solvent, while panels **C** and **D** in the DMF solvent.

4. Calculate the FRET Rate:

When determining the Förster resonance energy transfer (FRET) rate, we can employ two primary methods: the steady-state method and the fluorescence lifetime method[2]. The steady-state method measures the spectral overlap between donor and acceptor molecules, which is indicative of the potential for energy transfer (as shown in Figure S4). However, this method is sensitive to variations in concentration and sample conditions, potentially affecting the results.

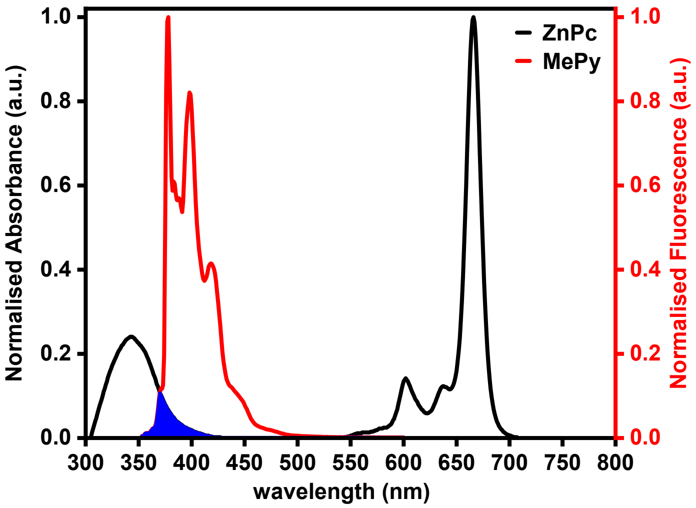

Figure S5: Overlap (Blue) of **ZnPc** normalised absorbance (Black) and **MePy** normalized fluorescence (Red) spectra in THF.

In contrast, the fluorescence lifetime method is considered more reliable and accurate for quantifying FRET. This approach takes into account dynamic factors such as molecular orientation and distance changes between donor and acceptor molecules and relies on the intrinsic photophysical properties of the molecules involved.

The energy transfer efficiency (E) can be experimentally calculated using fluorescence lifetimes through the following equation[3]:

$$E = 1 - (\tau_{DA} / \tau_D),$$

In this equation, τ_{DA} (0.3 ns) denotes the fluorescence lifetime of the donor/acceptor **ZnPcPy**, while τ_D (17.3 ns) represents the fluorescence lifetime of the donor **Py**. The resulting energy transfer efficiency is calculated to be 98%.

Deciding for the fluorescence lifetime method to quantify FRET ensures a more accurate and reliable evaluation of the energy transfer process. The degree of overlap between the spectra in **Figure S5** is critical for FRET to occur, as it indicates the potential for energy transfer between donor and acceptor molecules.

5. Cyclic Voltammetry (CV)

The redox properties of **ZnPc**, **MePy**, **ZnPcPy** and the mixture **ZnPc** + **MePy** were thoroughly investigated using cyclic voltammetry within the electrochemical window of $TBAPF_6$/THF at room temperature. The comprehensive electrochemical data can be found in **Table S1**, while the representative cyclic voltammograms are displayed in **Figure S6**.

Upon examination, it is clear that **ZnPc** exhibits two oxidation peaks at 0.61 V and 0.83 V, as well as two reduction peaks at -0.83 V and -1.15 V within the studied potential window. As the zinc metal is known to be electrochemically active, the redox couple processes are anticipated to occur on the phthalocyanine ring[4] . This observation is further corroborated by the smaller peak-to-peak separation between the first and second reduction peaks, which is less than 0.6 V[5].

Additionally, the cyclic voltammogram of **MePy** displays a reduction peak at a potential of -0.78 V. When **MePy** is combined with **ZnPc**, the resulting cyclic voltammogram exhibits two oxidation peaks at 0.58 V and 0.89 V and two reduction peaks at -0.86 V and -1.15 V. These reduction peaks can be attributed to the overlapping **Py** with the first **Pc** reduction and the second **Pc** reduction, respectively. The incorporation of **MePy** into the **ZnPc** system serves to enhance the electron density, rendering the mixture more easily oxidized and more resistant to reduction in comparison to **ZnPc** alone.

Furthermore, **ZnPcPy** and the mixture (**MePy** + **ZnPc**) demonstrate nearly identical two oxidation and reduction peaks, as illustrated in **Figure S6** and summarized in **Table S1**. This finding serves to strengthen the overall results section by highlighting the similarities in redox behavior between the mixture and the covalently linked compound.

Table S1. Voltametric data of **ZnPc**, **MePy**, **ZnPcPy**, and the mixture of **ZnPc** + **MePy** versus SCE.

Compound	$E_{1/2}$ ^{Oxd_1}/V	$E_{1/2}$ ^{Oxd_2}/V	$E_{1/2}$ ^{red_1}/V	$E_{1/2}$ ^{red_2}/V
ZnPc	0.61	0.83	-0.83	-1.15
MePy	-	-	-0.78	-
ZnPcPy	0.57	0.89	-0.85	-1.15
ZnPc + MePy	0.58	0.89	-0.86	-1.15

$E_{1/2}$ values were calculated as the average of anodic peak potential (E_{pa}) and cathodic peak potential (E_{pc}), represented by the formula $E_{1/2} = ((E_{pa} + E_{pc})/2)$, and referenced against SCE at a scan rate of 100 mV s^{-1}.

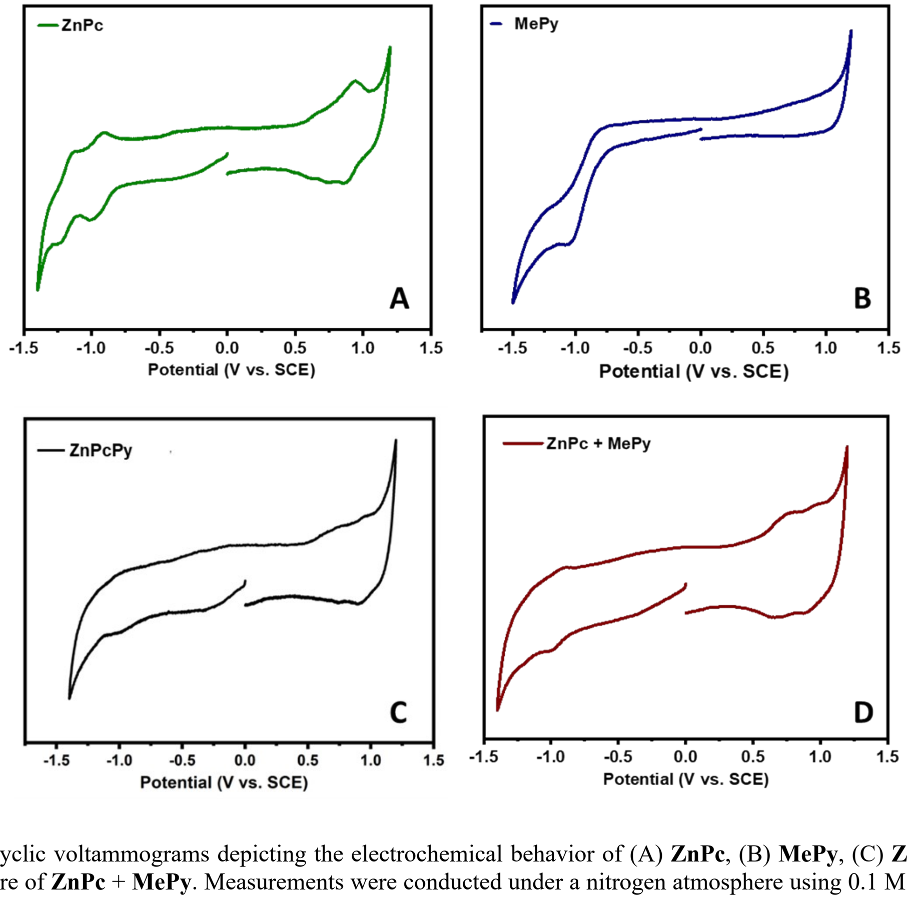

Figure S6: Cyclic voltammograms depicting the electrochemical behavior of (A) **ZnPc**, (B) **MePy**, (C) **ZnPcPy**, and (D) the mixture of **ZnPc** + **MePy**. Measurements were conducted under a nitrogen atmosphere using 0.1 M $TBAPF_6$ as the supporting electrolyte, with a scan rate of 100 mV/s.

6. Instrumentation:

All analyses were carried out in the Research Sector Projects Unit (RSPU) at Kuwait University, Durham University, and Northumbria University. Absorption UV-Vis studies were performed on an Agilent CARY 60 UV-Vis spectrometer. Steady-state and fluorescence measurements were performed at room temperature using a Horiba QM spectrofluorometer equipped with a 75 W Xenon lamp, with samples excited at 345 nm and 615 nm.

Fluorescence quantum yields (Φ_F) were determined using an integrating sphere incorporated into a spectrofluorometer (FLS980, Edinburgh Instruments) in THF, applying the following Equations[6]:

$$\Phi_F^X = \frac{L_{sam}}{E_{ref} - E_{sam}} \, (\%)$$

corrected to re-absorption:

$$\Phi_F = \frac{\phi_F^A}{1 - a \, + \, a \, . \, \Phi_F^X \, / \, 100} \, (\%)$$

In these equations, L_{Sam} represents the area under the detected spectrum where sample emission occurs, E_{Ref} is the area under the reflection portion of the detected spectrum using pure solvent as reference material (diffuse reflectance), E_{Sam} is the area under the reflection portion of the detected spectrum after absorption by the sample, and a is the reabsorbed area.

Time-resolved spectroscopy measurements were performed using the time-correlated single-photon counting technique (TCSPC) integrated into Edinburgh Instruments' FLS-

980 fluorescence spectrometer. The instrument was equipped with a Supercontinuum Fianium White Laser as an excitation source at 615 nm (frequency of 10 MHz, pulse width of 6 ps), and a Picosecond Pulsed Light Emitting Diode for excitation at 345 nm (frequency of 5 MHz, pulse width of ≈ 800 ps). The instrument response function was measured using a diffusive reference sample (LUDOX$_{®}$ from Sigma-Aldrich). Reconvolution fit analysis software (FLS980, Edinburgh Instruments) was employed for lifetime data analysis.

7. Transient absorption measurements:

Transient absorption measurements were conducted using an Edinburgh Instruments LP980 laser flash photolysis system in argon-saturated solutions, which were prepared by bubbling with argon for a minimum of 20 minutes. The excitation source was a Continuum Surelite laser coupled with an optical parametric oscillator (λ_{ex} = 345 nm and 615 nm). A pulsed Xenon lamp served as the analyzing light source. The laser and analyzing light beams intersected perpendicularly within a quartz cell featuring a 10 mm optical path length. The resulting signal was displayed and recorded via a Tektronix MDO 3022 Mixed Domain Oscilloscope and a PMT-LP detector. The PMT and monochromator configuration was employed for time-resolved data acquisition, while an iCCD camera on a spectrograph facilitated spectral mode data collection. The laser energy incident on the sample was reduced to approximately 20 mJ per pulse with a spot size of 78.5 mm^2.

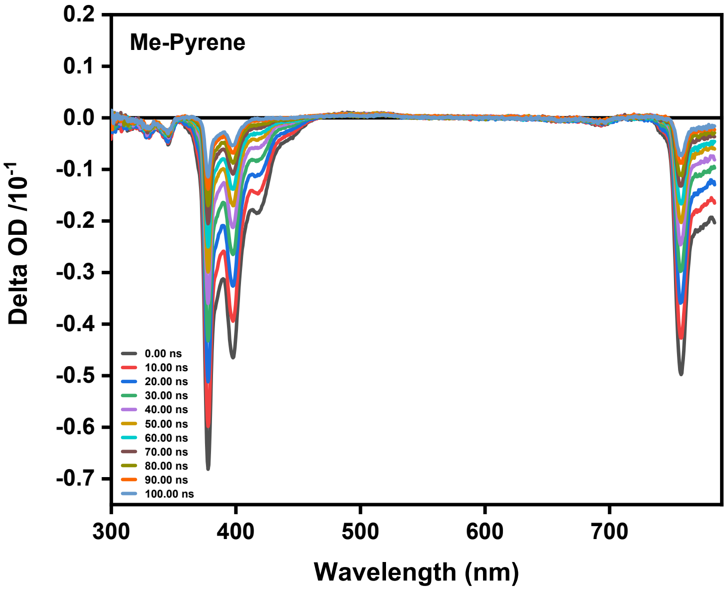

Figure S7: Transient absorption spectra of **MePy** excited at 345 nm.

8. Emission decay fitting

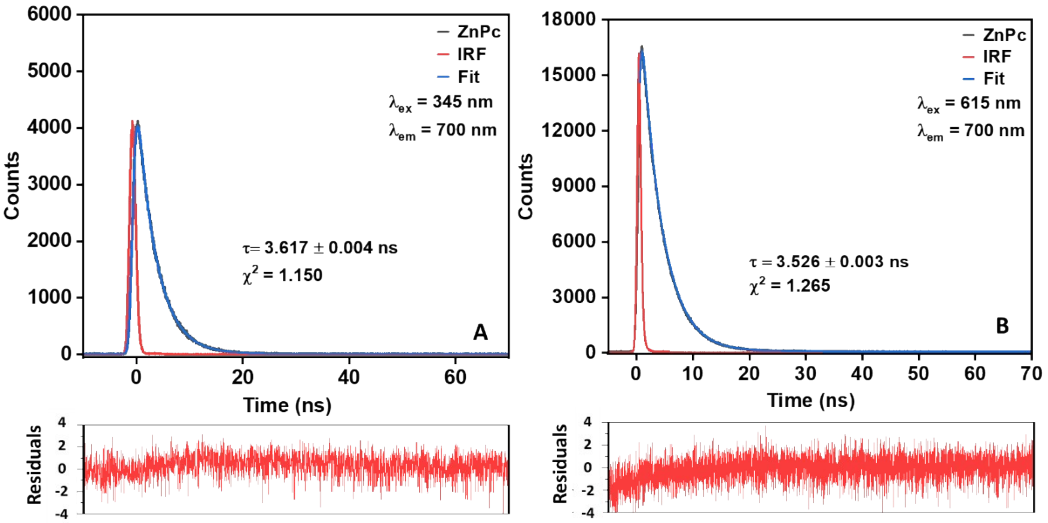

Figure S8: Fluorescence Decay (black), IRF (red), and Fitted Curve (blue) for **ZnPc**. (A) Excitation: 345 nm, Emission: 700 nm. (B) Excitation: 615 nm, Emission: 700 nm. Residuals of the fitting process are shown in the base plot.

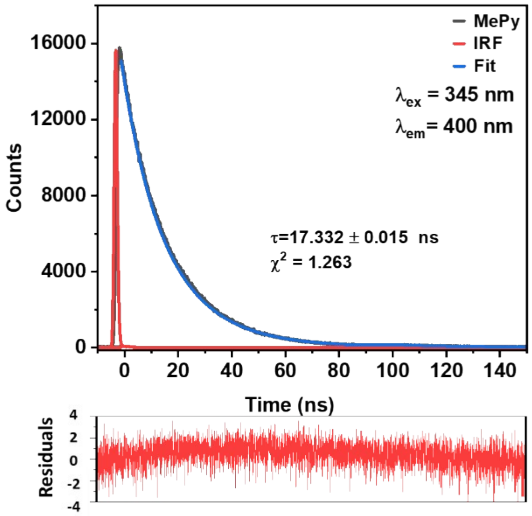

Figure S9: Fluorescence Decay (black), IRF (red), and Fitted Curve (blue) for **MePy**. Excitation: 345 nm, Emission: 400 nm. Residuals of the fitting process are shown in the base plot.

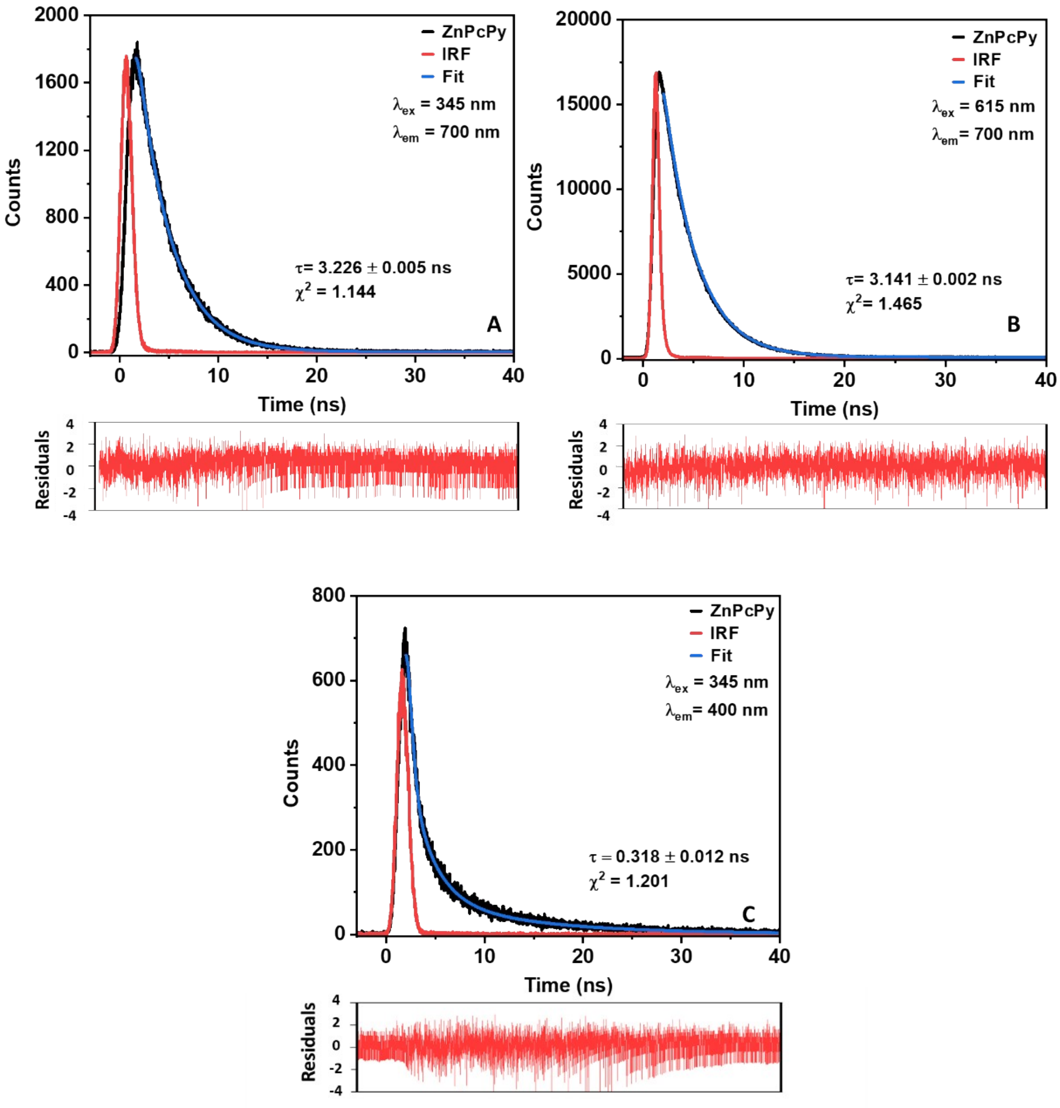

Figure S10: Fluorescence Decay (black), IRF (red), and Fitted Curve (blue) for **ZnPcPy**. (A) Excitation: 345 nm, Emission: 700 nm. (B) Excitation: 615 nm, Emission: 700 nm. (C) Excitation: 345 nm, Emission: 400 nm. Residuals of the fitting process are shown in the base plot.

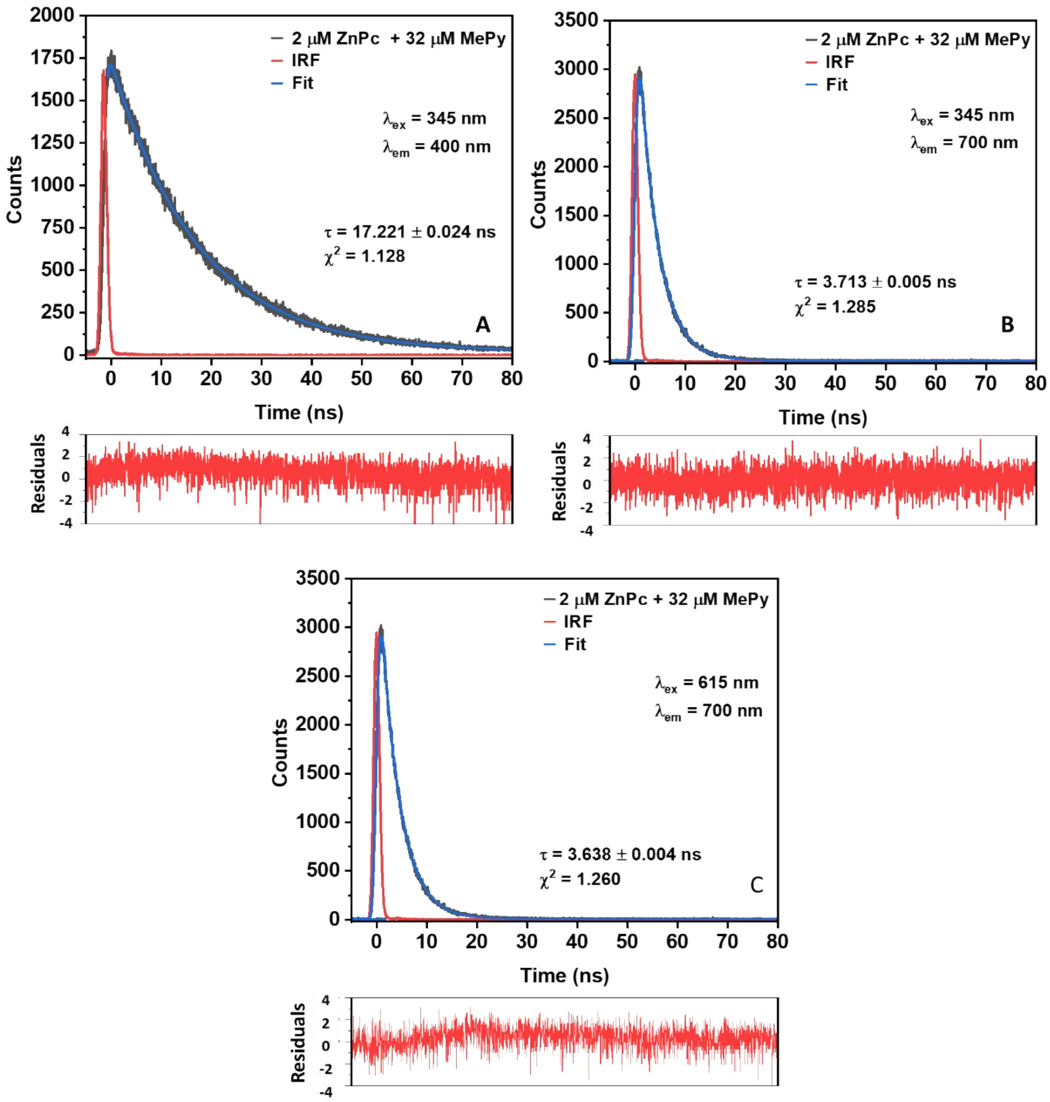

Figure S11: Fluorescence Decay (black), IRF (red), and Fitted Curve (blue) for the mixture of **2μM ZnPc + 32 μM MePy**. (A) Excitation: 345 nm, Emission: 400 nm. (B) Excitation: 345 nm, Emission: 700 nm. (C) Excitation: 615 nm, Emission: 700 nm. Residuals of the fitting process are shown in the base plot.

9. References

1. Husain, A.; Ganesan, A.; Sebastian, M.; Makhseed, S., Large ultrafast nonlinear optical response and excellent optical limiting behaviour in pyrene-conjugated zinc (II) phthalocyanines at a near-infrared wavelength. *Dyes and Pigments* **2021,** *184*, 108787.
2. Dou, S.; Wang, Y.; Zhang, X., Amphiphilic Fluorescence Resonance Energy-Transfer Dyes: Synthesis, Fluorescence, and Aggregation Behavior in Water. *Chemistry–A European Journal* **2020,** *26* (50), 11503-11510.
3. Lakowicz, J. R., *Principles of fluorescence spectroscopy*. Springer: 2006.
4. Sekota, M.; Nyokong, T., Cyclic voltammetry and spectroelectrochemistry of osmium phthalocyanines in aqueous and non-aqueous solvents. *Polyhedron* **1996,** *15* (17), 2901-2908.
5. Leznoff, C.; Lever, A., Properties and Applications. *VCH New York* **1989**.
6. Lagorio, M. G., Determination of fluorescence quantum yields in scattering media. *Methods and Applications in Fluorescence* **2020,** *8* (4), 043001.